A Research on the Load Calculation Method in Designing the Traction Power Supply for Integrated Subway – MCR

Dong Doan Van
Science and Technology Application for Sustainable Development Research Group, Ho Chi Minh City University of Transport, Vietnam
dongdv@ut.edu.vn (corresponding author)

Received: 4 April 2023 | Revised: 20 April 2023 | Accepted: 24 April 2023

 DOI: https://doi.org/10.48084/etasr.5909

ABSTRACT

This paper presents a load calculation method in the design of a traction power supply for integrated subways. Integrated subways have a large carrying capacity and the ability to balance between meeting travel needs and satisfying conditions such as high quality service, cost optimization for railway infrastructure construction, and installation of traction power systems. In an integrated model, the calculation of the traction power supply design is much more complicated than in other stand-alone models. This paper presents the research results on the load calculation method of a traction power supply for the operation of the system. The results show the feasibility of the method when applied to an asynchronous loading system and met the standards of IEEE P1653.2, EN 50328, and IEC 60146-1 in the design of the power supply for permitted overloads according to class VI.

Keywords-urban rail transit; integrated urban railway; traction power supply; integrated subway

I. INTRODUCTION

A sustainable integrated urban transport n integrated system, with the large-scale interaction of various public transportation modes, attracts users with its friendliness, comfort, and time- and cost- saving in commuting and providing full "door-to-door" public transportation services. Urban rail is an indispensable part of a sustainable integrated urban transport system. However, different integrated solutions have been recommended depending on the type of transportation. A system with a large transport capacity integrating subway and suburban railway is needed to meet the large commuting needs connecting suburban areas and city centers. This system should operate with a very high transport capacity during peak hours, which is difficult to achieve separately for each type of transportation, and return to normal operating conditions during non-peak hours with low construction investment cost. The benefits of an integrated subway system are highlighted in [1-4]. To ensure that the system operates as flexibly, optimally, reliably, and energy-efficiently as desired, it needs to have a strong power supply system to meet the highest transport capacity during peak hours. However, most past studies focused on planning, forecasting, and addressing transport capacity, energy saving, and evaluating the benefits it brings to the comprehensive development of smart cities under the new context of integrated subways [5-10]. Therefore, this study focuses on calculating the design load for the power supply to enable the flexible operation of the system according to IEEE P1653.2, EN 50328, and IEC 60146-1 standards with an allowable overload of up to level VI. Matlab R2017b/Railway Systems software was used for computations and simulations.

II. INTEGRATED LOAD CALCULATION METHOD

A. Integrating Subway and Suburban Railway.

Integrated subway (ME) and suburban railway (CR) is a method of combining the transportation capacity of suburban railways by operating on subway travel corridors during peak hours (MCR). This method allows increased transportation capacity and service frequency without the need to increase the number of trains operating on it. On the other hand, suburban trains operate like subway trains when running on the line. Figure 1 describes the integrated train running chart, in which A to E are the terminal stations of the subway line, B to E (or B to A but stops at any station) the terminal stations of the suburban railway, and B to A is the integrated peak-hour suburban railway station. Therefore, with this capability, passengers can travel continuously from the suburbs to the city center and stop at any station without having to change lines. At the same time, using suburban trains to meet the required number of trains during peak hours reduces the cost of purchasing train fleets. This is a typical example of integration: if the individual frequency for each type is 300s (a train appears at each station every 300s), then it will be 150s (a train appears at each station every 150s) when combined in an interleaved manner. If not integrated, relying on the combination of suburban trains stopping at all stations for the demand of subway transportation, the service frequency (headway) of the subway trains would need to be increased to

meet the demand, increasing the number of trains running on the section and the trains in reserve, which increases all related costs, such as purchasing trains, operation, maintenance, etc.

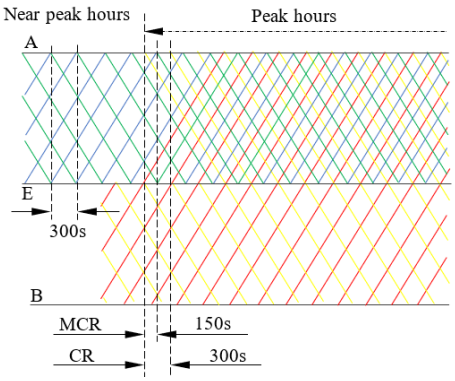

Fig. 1. The integrated train running chart during peak hours.

B. Load Calculation Method

There are many methods to calculate the design load for supplying electric traction power to subway or suburban railway systems [11-20]. However, these methods allow separate calculations for each system. For an integrated system, which is a combination of two systems with different capacities on the same power supply system, the difference is the train load, which is an important issue in load calculations. As the carrying capacities of subway and suburban railway systems are different, the train current used is also different. Correspondingly, the mechanical resistance (Rr), the acceleration resistance (Ra), acceleration, and operation speed are also different. The result is that the maximum instantaneous traction force for each train trip between two passenger stations is different. For a train to move, it needs to be provided with a basic force to change its velocity from a stationary state to motion with maximum acceleration. This force is called the necessary traction force (F_t) that must overcome the forces of mechanical resistance (F_{Rr}) and acceleration resistance (F_{Ra}) caused by the mass of the train (M) moving linearly on the track.

$$F_t = F_{Ra} + F_{Rr} \quad (1)$$

Equation (1) is also affected by additional or simultaneous different resistance components based on the railroad grade profile (F_{Rc}, F_{Rg}, F_{Rt}) on a power supply section of a traction substation (TPS). The maximum required traction force from (1) can be rewritten as follows:

$$F_{t\text{-}max} = F_{Ra} + \sum F_R \quad (2)$$

Figure 2 shows the number of trains appearing within the power supply radius of a traction substation based on the integrated train operation chart. With a service frequency of 150s, determined by the running speed and the power supply radius, there are always more than 4 trains operating continuously in both directions that require power supply. By relying on the service frequency (n_f - trains/hour/direction), running speed (v_{sc} - km/h), and power supply radius (DTPS - km), the total number of trains appearing within this range can be determined as n_k trains/direction. Therefore, the total train load that the power needs to supply in both directions can be calculated.

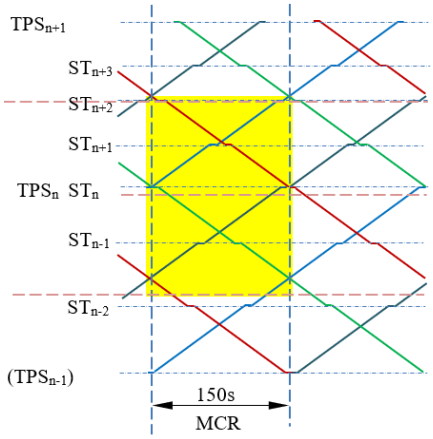

Fig. 2. Peak hour integrated train operation diagram within the scope of a traction substation.

The weight of train x (M_x) during peak hours is calculated as the weight of the locomotive and the total weight of the cars, where n_x is the number of locomotives and m_x is the number of cars.

$$M_x = n_x \cdot M_{d,x} + m_x \cdot M_{c,x} \quad (3)$$

$$M_{d,x} = \left(p_{d,x} \cdot f_{s.d,x} \cdot S_{d,x} + f_{d,x}\right) \cdot m_p + m_{d,x} \quad (4)$$

$$M_{c,x} = \left(p_{c,x} \cdot f_{s.c,x} \cdot S_{c,x} + f_{c,x}\right) \cdot m_p + m_{c,x} \quad (5)$$

with criteria:

$$\begin{cases} 4 < p_{d,x} \le 7,\ p/m^2 \\ 4 < p_{c,x} \le 7, p/m^2 \\ 1 < n_x \le 2,\ n_x \in Z_+ \\ 1 \le m_x,\ m_x \in Z_+ \\ n_x \cdot l_{d,x} + m_x \cdot l_{c,x} \le l_{st\text{-}min} \end{cases} \quad (6)$$

The weight of train y during peak hours is given by:

$$M_y = n_y \cdot M_{d,y} + m_y \cdot M_{c,y} \quad (7)$$

$$M_{d,y} = \left(p_{d,y} \cdot f_{s.d,y} \cdot S_{d,y} + f_{d,y}\right) \cdot m_p + m_{d,y} \quad (8)$$

$$M_{c,y} = \left(p_{c,y} \cdot f_{s.c,y} \cdot S_{c,y} + f_{c,y}\right) \cdot m_p + m_{c,y} \quad (9)$$

with criteria:

$$\begin{cases} 4 < p_{d,y} \le 7,\ p/m^2 \\ 4 < p_{c,y} \le 7, p/m^2 \\ 1 < n_y \le 2,\ n_y \in Z_+ \\ 1 \le m_y,\ m_y \in Z_+ \\ n_y \cdot l_{d,y} + m_y \cdot l_{c,y} \le l_{st\text{-}min} \end{cases} \quad (10)$$

The components of train motion resistance within the power supply range of any traction substation i and along the j-th station route are:

Mechanical Resistance:

$$R_{r.x,y} = A + B \cdot v + C \cdot v^2 \quad (11)$$

Road curve [17]:

$$\begin{cases} R_{c.i,j} = \frac{650}{r-55}, & r < 300 \\ R_{c.i,j} = \frac{500}{r-30}, & r \geq 300 \end{cases} \quad (12)$$

Slope:

$$R_{g.i,j} = \pm G/1000 \quad (13)$$

Tunnel:

$$R_{t.i,j} = \frac{f_t \cdot v^2}{W} \quad (14)$$

Acceleration drag:

$$R_{a.x,y.i,j} = \frac{a \cdot \xi}{g} \quad (15)$$

The maximum resistance depends on the grade profile:

$$\begin{cases} \sum R_{i,j} = R_{ci,j} + R_{gi,j} + R_{ti,j} \\ R_{max.i,j} \leq \sum R_{i,j} < R_a + R_r \end{cases} \quad (16)$$

The maximum instantaneous tractive force of trains *x*, *y* in each direction, within the supply range of a traction substation *i* and the route to the j^{th} station in the forward (*h*) and the backward directions (*k*) is:

$$F_{ti,j\text{-}kx,max} = M_x \cdot \left(R_{a,x} + R_{r,x} + \sum R_{max,j\text{-}kx}\right) \quad (17)$$

$$\sum R_{max,j\text{-}kx} = R_{c,j\text{-}kx} + R_{g,j\text{-}kx} + R_{t,j\text{-}kx} \quad (18)$$

$$F_{ti,j\text{-}hx,max} = M_x \cdot \left(R_{a,x} + R_{r,x} + \sum R_{max,j\text{-}hx}\right) \quad (19)$$

$$\sum R_{max,j\text{-}hx} = R_{c,j\text{-}hx} + R_{g,j\text{-}hx} + R_{t,j\text{-}hx} \quad (20)$$

$$F_{ti,j\text{-}ky,max} = M_x \cdot \left(R_{a,y} + R_{r,y} + \sum R_{max,j\text{-}ky}\right) \quad (21)$$

$$\sum R_{max,j\text{-}ky} = R_{c,j\text{-}ky} + R_{g,j\text{-}ky} + R_{t,j\text{-}ky} \quad (22)$$

$$F_{ti,j\text{-}hy,max} = M_x \cdot \left(R_{a,y} + R_{r,y} + \sum R_{max,j\text{-}hy}\right) \quad (23)$$

$$\sum R_{max,j\text{-}hy} = R_{c,j\text{-}hy} + R_{g,j\text{-}hy} + R_{t,j\text{-}hy} \quad (24)$$

Assuming that the integrated system operates with an equal service frequency for both *x* and *y* train lines on the route, the total maximum instantaneous traction force is determined based on the maximum instantaneous traction force in the power supply segment of an electric traction station in both directions, as follows:

$$\sum_{i=1}^{1} F_{ti,j,\,(na)max} = 2 \cdot \sum_{na.\ p_l \in i,j} p_{l,max} \cdot F_{ti,j\{kx,hx,ky,hy\},max} \quad (25)$$

In (24), it depends on the maximum allowable frequency $c_{1,max}$ of the transmission line:

$$\begin{cases} \sum_{na.\ p_l \in i,j} p_{l,max} = \frac{60}{c_{l,max}} \cdot \frac{D_{TPSi}}{v_{sc}} \\ 1.5 \leq c_{l,max} < c_{l,ME},\ c_{l,max} = \frac{C_{p,max}}{C_{t,max}} \end{cases} \quad (26)$$

If there is a power outage at any substation disrupting the power supply, then:

$$\sum_{i=1}^{i+\frac{1}{2}} F_{ti,j,\,(er),max} = 2 \cdot \sum_{er.p_l \in i,j} p_{l,max} \cdot F_{ti,j\{kx,hx,ky,hy\},max} \quad (27)$$

where:

$$\begin{cases} \sum_{er.\ p_l \in i,j} p_{l,max} = \frac{60}{c_{l,max}} \cdot \frac{1}{v_{sc}} \cdot \left[D_{TPSi} + \frac{D_{TPS(i+1)}}{2}\right] \\ 1.5 \leq c_{l,max} < c_{l,ME},\ c_{l,max} = \frac{C_{p,max}}{C_{t,max}} \end{cases} \quad (28)$$

Based on the force-velocity curve, the instantaneous maximum power requirement is calculated as a function of the force-velocity relationship. The power under normal operating conditions (na) and during an error (er) is:

$$P_{ti,j(na)max} = \sum_{i=1}^{p_{l(na),max}} F_{ti,j,\,(na)max} \cdot \frac{v}{3.6 \cdot \eta_{mc} \cdot \eta_{mt}} \quad (29)$$

$$P_{ti,j(er)max} = \sum_{i=1}^{p_{l(er),max}} F_{ti,j,\,(er)max} \cdot \frac{v}{3.6 \cdot \eta_{mc} \cdot \eta_{mt}} \quad (30)$$

with mechanical (η_{mc}) and motor efficiency (η_{mt}) conditions:

$$\begin{cases} \eta_{mc,min} < \eta_{mc} \leq \eta_{mc,max} \\ \eta_{mt,min} < \eta_{mt} \leq \eta_{mt,max} \\ v_{sc} < v \leq v_{peak} \end{cases} \quad (31)$$

The auxiliary consumption power used for purposes other than pulling force on each train type is calculated as follows:

$$P_{[x,y],i(na)aux} = \sum_{na.\ p_l \in i} p_{l,max} \cdot \left(n_{[x,y]} \cdot p_{d,[x,y]} + m_{[x,y]} \cdot p_{c,[x,y]}\right) \quad (32)$$

$$P_{[x,y],i(er)aux} = \sum_{er.\ p_l \in i} p_{l,max} \cdot \left(n_{[x,y]} \cdot p_{d,[x,y]} + m_{[x,y]} \cdot p_{c,[x,y]}\right) \quad (33)$$

The maximum power consumption under normal operating conditions and when an error occurred at station *i* are calculated as:

$$P_{TPSi(na)max} = P_{ti,j(na)max} + P_{[x,y],i(na)aux} \quad (34)$$

$$P_{TPSi(er)max} = P_{ti,j(er)max} + P_{[x,y],i(er)aux} \quad (35)$$

Equations (36) and (37) give the maximum power consumption required to be supplied if there is regenerative braking (energy returned during braking) under normal operating conditions and when an error occurres The percentage of the energy recovered (η_{re}) depends on the frequency of service and the voltage of the traction system:

$$P_{TPSi(re,\,na)max} = P_{TPSi(na)max}\left(1 - \eta_{re}\right) \quad (36)$$

$$P_{TPSi(re,er)max} = P_{TPSi(er)max}\left(1 - \eta_{re}\right) \quad (37)$$

With the condition based on the type of service:

$$\begin{cases} \eta_{re,na.\ min} < \eta_{re[x,y]} \leq \eta_{re,na,.max} \\ \eta_{re,er.\ min} < \eta_{re[x,y]} \leq \eta_{re,er.max} \end{cases} \quad (38)$$

the power selection for the traction substation is:

$$P_{TPSi(er,na)max} \leq P_{TPSi(na),\,min} \quad (39)$$

$$P_{TPSi(re,\,er)max} \leq P_{TPSi(re),min} \quad (40)$$

The power of the traction substation selected according to (35) and (36) must comply with the IEEE P1653.2, EN 50328, and the IEC 60146-1 standards.

III. SYSTEM DESIGN

A. Load Parameters

TABLE I. THE PROFILE OF THE ROUTE FROM TRACTION SUBSTATION NO. 3 TO NO. 4 ALONG THE LINE

Km	*TPSi*	*STj*	*G‰*	*C*	*Rt*
10.0	SP	11			
11.00		12			
11.50			+35	650	
12.00		13			
12.40	3				
13.20		14			
13.70			+5	500	
14.00	SP				
14.40		15			
15.40		16	-5		17.14
15.80			-20		17.14
16.00	4				17.14
16.40		17			17.14
17.40		18			17.14

TABLE II. LOAD PARAMETERS

Symbol	Units	Value
$C_{L.p1}$	[p/h/d]	45,000
$C_{L.p2}$	[p/h/d]	54,000
$a_{x,max}/\beta_{x,max}$	[m/s^2]	0.9/1.0
$a_{y,max}/\beta_{y,max}$	[m/s^2]	0.85/1.0
R_x,R_y	[kg/ton]	
$R_x = 3.25 + 0.039 \cdot V + 0.000659 \cdot V^2$		
$R_y = 2.45 + 0.044 \cdot V + 0.000374 \cdot V^2$		
v_{sc},v_{max}	[km/h]	45/60
Train load *Ix*[*A*]: 400·(4*M*)+200·(2*M*)+200·(2*Mc*)		
Train load [*A*]: 400·(4*M*)+200·(1*M*)+200·(2*Mc*)		
Support load Iaux [*A*]: 25.3333·(6*M*)+24·(2*Mc*)		
Support load Iauy [*A*]: 26.6667·(5*M*)+24·(2*Mc*)		

TABLE III. TRAIN LOAD PARAMETERS

Symbol	Specifications	Description
$C_{p1;2}$	45,000; 54,000	Person/hour/direction
n_x, n_y	2; 2	Control car
m_x, m_y	6; 5	Locomotive unit
$m_{d,x;y}$	40 tons; 42 tons	Control car
$_{mc,x;y}m_{c,x;y}$	38 tons; 41 tons	Locomotive unit
$S_{d,x}$	3.2x22m^2	The floor area of a passenger car
$S_{c,x}$	3.2x23m^2	Passenger area
$S_{d,y}$	3.27x25m^2	The floor area of a passenger car
$S_{c,y}$	3.27x26m^2	Passenger area
$f_{s.d,x;y}$	0.45%; 0.42%	Occupancy rate
$f_{s.c,x;y}$	0.55%; 0.45%	Occupancy rate
$f_{d,x}$	38 seats	Cabin seat
$f_{c,x}$	44 seats	Passenger seat
$f_{d,y}$	32 seats	Cabin seat
$f_{c,y}$	42 seats	Passenger seat
m_p	55kg	Weight/passenger

B. Load Calculation Process

The flowchart of the load calculation process is shown in Figure 3.

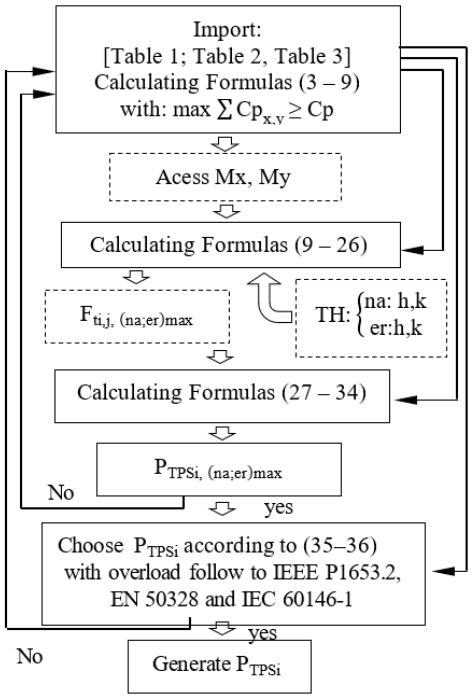

Fig. 3. Flowchart of the load calculation process.

IV. RESULT AND DISCUSSION

A. Results of Load Calculations

The train parameters that have the carrying capacity to meet the demand of the line described in Table III are selected. The trains have the maximum passenger capacity including fixed seats and standing passengers of 7p/m^2 in both stages. In stage 1, the demand for transportation is 45,000p/h/d and the supply capacity is 45,774p/h/d with a headway of 3p/t/d. In stage 2, the demand for transportation is 54,000p/h/d and the supply capacity is 54,929p/h/d with a headway of 2.5p/t/d. To meet the different demands in each stage in this design, the system only changes the service frequency (the time interval between train services) without changing the structure or carrying capacity. Therefore, with the maximum carrying capacity according to the stages, the subway train *x* weighs 224.97 tons and the suburban train *y* weighs 211.68 tons.

B. Calculation Results of Traction Force

Consider a section of the line between two traction substations with a complex railway track from station ST11 to ST18, as shown in Table I. Under normal operation, TPS3 supplies power from station ST11 to ST14, while TPS4 supplies power from station ST15 to ST18. Assuming that TPS4 experiences a disruption in its power supply, TPS3 will have to provide power to its section and a portion of the adjacent station, from station ST11 to ST16. The following scenarios may occur:

In case 1, the traction force and train speed curves vary depending on whether the train is moving in the direction of the power supply or the opposite one. In normal operation, when both TPS3 and TPS4 are supplying power to the trains, the maximum required traction force is reached when the trains

accelerate in both the forward and backward directions at the stations. The maximum required traction force for the outer suburban train $F_{y,na.max}$ is 205.69kN, and for the metro train $F_{x,na.max}$ is 233.46kN. In the event of a TPS4 power outage, TPS3 is required to supply power to the trains along its section as well as a part of the adjacent substation from ST11 to ST16. The maximum required traction force for the suburban train $F_{y,er.max}$ is 216.07kN, and for the metro train $F_{x,er.max}$ is 244.5kN. Overall, in case 1, the curves of traction force and train speed are relatively similar for both the outer suburban and metro trains. The maximum required traction force increases slightly in the event of a TPS4 power outage, but the difference is not significant. The train speed also changes slightly within the power supply range of a traction substation, but this change is not enough to impact the train operation.

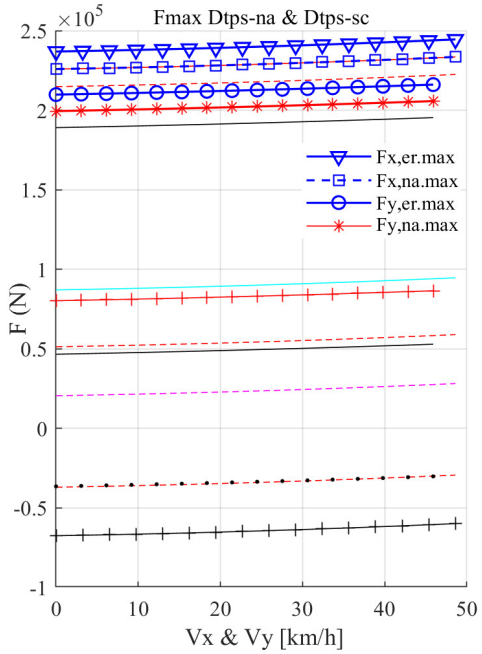

Fig. 4. Comparison of the traction force and train speed curves within the power supply range of a traction substation in case 1.

In case 2, both TPS3 and TPS4 supply power to trains operating on the interacting section. The required traction force distribution in the described section is shown in Figure 5. Under normal operating conditions, TPS3 supplies power only to the traction force required when the train accelerates at the departure and arrival stations of the suburban train. The maximum required traction force for the suburban train $F_{y,na.max}$ is 205.69kN. In the event of a TPS3 malfunction, it must supply power to the required traction force for the train acceleration at the departure and arrival stations in the tunnel. The maximum required traction force for the suburban train $F_{y,er.max}$ is 216.07kN and for the subway train $F_{x,er.max}$ is 244.5kN. In terms of speed, when TPS4 is in normal operation, it supplies power to the trains in the described section. Therefore, the speed curve is smooth and not affected by the power supply. However, in the event of a TPS4 malfunction, the power supply to the trains in this section will be affected, which may result in a decrease in their speed.

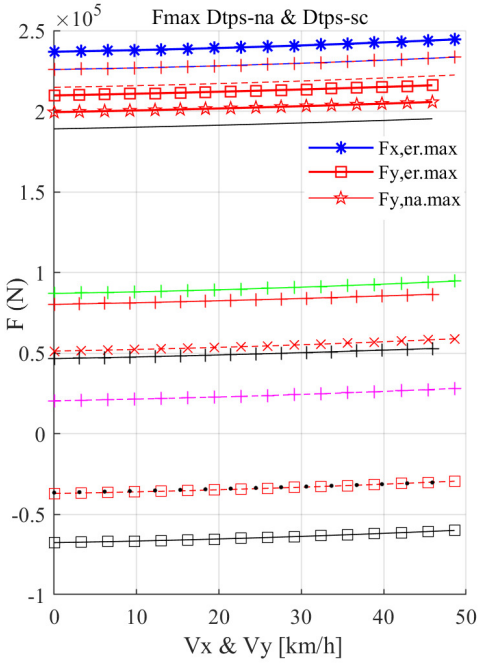

Fig. 5. Comparison of the force and speed curves of trains within the power supply range of an electric traction station in case 2.

V. CONCLUSION

This paper presented the results of a study on a method for calculating the maximum instantaneous pulling force to predict the instantaneous power consumption of loads for the design of power stations in integrated subway train models - MCR. The method was designed and simulated using Matlab R2017b/Railway Systems software, with a variety of load cases for maximum power consumption during peak hours in different stages and different situations to demonstrate its reliability. In addition, the method also demonstrates transparency and logic in calculating data according to a sequence with filtering and comparison for contingency situations to avoid power wastage. The calculated power compared to the minimum and maximum load requirements was 14.67% and 21.81%, which is suitable for station power that meets the standards of IEEE P1653.2, EN 50328, and IEC 60146-1 for redundancy coefficients. Finally, the proposed method of calculation is a reliable and cost-effective scientific approach in the study of designing the power supply for subway trains.

REFERENCES

[1] Y. Zhou, H. Yang, Y. Wang, and X. Yan, "Integrated line configuration and frequency determination with passenger path assignment in urban rail transit networks," *Transportation Research Part B: Methodological*, vol. 145, pp. 134–151, Mar. 2021, https://doi.org/10.1016/j.trb.2021.01.002.

[2] W. Kampeerawat and T. Koseki, "Integrated Design of Smart Train Scheduling, Use of Onboard Energy Storage, and Traction Power Management for Energy-Saving Urban Railway Operation," *IEEJ*

Journal of Industry Applications, vol. 8, no. 6, pp. 893–903, 2019, https://doi.org/10.1541/ieejjia.8.893.

[3] W. Kampeerawat and T. Koseki, "Efficient Urban Railway Design Integrating Train Scheduling, Wayside Energy Storage, and Traction Power Management," *IEEJ Journal of Industry Applications*, vol. 8, no. 6, pp. 915–925, 2019, https://doi.org/10.1541/ieejjia.8.915.

[4] T. Kara and M. C. Savas, "Design and Simulation of a Decentralized Railway Traffic Control System," *Engineering, Technology & Applied Science Research*, vol. 6, no. 2, pp. 945–951, Apr. 2016, https://doi.org/10.48084/etasr.631.

[5] N. Zhao, C. Roberts, S. Hillmansen, Z. Tian, P. Weston, and L. Chen, "An integrated metro operation optimization to minimize energy consumption," *Transportation Research Part C: Emerging Technologies*, vol. 75, pp. 168–182, Feb. 2017, https://doi.org/10.1016/j.trc.2016.12.013.

[6] X. Luan, Y. Wang, B. De Schutter, L. Meng, G. Lodewijks, and F. Corman, "Integration of real-time traffic management and train control for rail networks - Part 2: Extensions towards energy-efficient train operations," *Transportation Research Part B: Methodological*, vol. 115, pp. 72–94, Sep. 2018, https://doi.org/10.1016/j.trb.2018.06.011.

[7] H. Liu, T. Tang, J. Lv, and M. Chai, "An integrated energy conservation model in subway systems," *Journal of Physics: Conference Series*, vol. 1176, no. 4, Nov. 2019, Art. no. 042042, https://doi.org/10.1088/1742-6596/1176/4/042042.

[8] S. Zhao, H. Yang, and Y. Wu, "An integrated approach of train scheduling and rolling stock circulation with skip-stopping pattern for urban rail transit lines," *Transportation Research Part C: Emerging Technologies*, vol. 128, Jul. 2021, Art. no. 103170, https://doi.org/10.1016/j.trc.2021.103170.

[9] S. Zhao, J. Wu, Z. Li, and G. Meng, "Train Operational Plan Optimization for Urban Rail Transit Lines Considering Circulation Balance," *Sustainability*, vol. 14, no. 9, Jan. 2022, Art. no. 5226, https://doi.org/10.3390/su14095226.

[10] X. Yang, A. Chen, X. Li, B. Ning, and T. Tang, "An energy-efficient scheduling approach to improve the utilization of regenerative energy for metro systems," *Transportation Research Part C: Emerging Technologies*, vol. 57, pp. 13–29, Aug. 2015, https://doi.org/10.1016/j.trc.2015.05.002.

[11] F. Mao, Z. Mao, and K. Yu, "The Modeling and Simulation of DC Traction Power Supply Network for Urban Rail Transit Based on Simulink," *Journal of Physics: Conference Series*, vol. 1087, no. 4, Jun. 2018, Art. no. 042058, https://doi.org/10.1088/1742-6596/1087/4/042058.

[12] V. V. S. K. Bhajana and P. Drabek, "Development and Evaluation of an Isolated Resonant Converter for Auxiliary Power Supply in DC Traction," *Engineering, Technology & Applied Science Research*, vol. 9, no. 2, pp. 4048–4052, Apr. 2019, https://doi.org/10.48084/etasr.2692.

[13] Z. Tian, N. Zhao, S. Hillmansen, S. Su, and C. Wen, "Traction Power Substation Load Analysis with Various Train Operating Styles and Substation Fault Modes," *Energies*, vol. 13, no. 11, Jan. 2020, Art. no. 2788, https://doi.org/10.3390/en13112788.

[14] J. Zhang, W. Liu, Z. Tian, H. Zhang, J. Zeng, and H. Qi, "Modelling, simulating and parameter designing for traction power system with bidirectional converter devices," *IET Generation, Transmission & Distribution*, vol. 16, no. 1, pp. 110–122, 2022, https://doi.org/10.1049/gtd2.12281.

[15] S. Razmjou and A. Younesi, "A Comprehensive DC Railway Traction System Simulator Based on MATLAB: Tabriz Line 2 Metro Project Case Study," *Journal of Operation and Automation in Power Engineering*, vol. 9, no. 2, pp. 144–159, Feb. 2021, https://doi.org/10.22098/joape.2021.8197.1569.

[16] Y. Chen, Z. Tian, S. Hillmansen, C. Roberts, and N. Zhao, "DC Traction Power Supply System Reliability Evaluation and Robust Design," in *2019 IEEE 3rd International Electrical and Energy Conference (CIEEC)*, Beijing, China, Sep. 2019, pp. 1153–1158, https://doi.org/10.1109/CIEEC47146.2019.CIEEC-2019424.

[17] Y. Chen, Z. Tian, C. Roberts, S. Hillmansen, and M. Chen, "Reliability and Life Evaluation of a DC Traction Power Supply System Considering Load Characteristics," *IEEE Transactions on Transportation Electrification*, vol. 7, no. 3, pp. 958–968, Sep. 2021, https://doi.org/10.1109/TTE.2020.3047512.

[18] S. Su, T. Tang, and Y. Wang, "Evaluation of Strategies to Reducing Traction Energy Consumption of Metro Systems Using an Optimal Train Control Simulation Model," *Energies*, vol. 9, no. 2, Feb. 2016, Art. no. 105, https://doi.org/10.3390/en9020105.

[19] A. Steimel, Electric Traction - Motive Power and Energy Supply: Basics and Practical Experience. Munich, Germany: Oldenbourg Industrieverlag, 2008.

[20] T. N. Le, H. M. V. Nguyen, T. A. Nguyen, T. T. Phung, and B. D. Phan, "Optimization of Load Ranking and Load Shedding in a Power System Using the Improved AHP Algorithm," *Engineering, Technology & Applied Science Research*, vol. 12, no. 3, pp. 8512–8519, Jun. 2022, https://doi.org/10.48084/etasr.4862.